High-Frequency Leaky-Mode Excitation on a Microstrip Line

Francisco Mesa, *Member, IEEE,* David R. Jackson, *Fellow, IEEE,* and Manuel J. Freire

***Abstract*—The excitation of leaky modes (LMs) and the continuous spectrum (CS) on microstrip line at high frequencies from a delta-gap source is studied. The delta-gap source models a practical source or discontinuity on the line. It is shown that the current excited from the source exhibits spurious effects at high frequencies due to the excitation of the CS (radiation spectrum), which may or may not be dominated by a physical LM, depending on the frequency range and the substrate permittivity. In some cases, the spurious effects are due to a physical LM, while in other cases the effects are due to the excitation of one or more "residual-wave" (RW) currents, which have not been previously studied for open microstrip lines. There are two types of RW currents: a free-space type and a surface-wave type. Depending on the frequency and the structural parameters, either of these may be the more dominant. At certain frequencies, weakly attenuated high-order LMs may also be excited, in which case spurious effects are observed out to large distances from the source.**

***Index Terms*—Continuous spectrum, crosstalk, leaky waves, microstrip, microwave integrated circuits, printed circuits.**

I. Introduction

THE existence of leaky modes (LMs) on printed circuit transmission lines has been well established for a variety of structures [1]–[19]. One of the most commonly used structures is the microstrip line. It was shown in [1] that an LM may exist on a microstrip line with an isotropic substrate at high frequencies, when the substrate thickness approaches roughly one tenth of a wavelength. It was also demonstrated experimentally in [1] that spurious transmission effects may occur on a microstrip line at high frequencies. These spurious effects include signal attenuation and significant oscillations in the current or voltage that is excited on the line by a source. In [1], these effects were attributed to the existence of an LM, although there was no direct evidence to support this, since only the propagation characteristics of the LMs on the infinite microstrip line were studied, and not the current excitation due to a practical source. In general, studying the propagation characteristics of an LM on an infinite line without a source does not provide quantitative information about the extent to which the mode will be excited by a practical source. Furthermore, studying only the infinite line does not reveal what other types of radiation effects from the source discontinuity may occur at high frequencies, in addition to the LM excitation.

Manuscript received April 2, 2001; revised August 23, 2001. This work was supported in part by the State of Texas under the Advanced Technology Program.

F. Mesa and M. J. Freire are with the Microwave Group, Department of Electronics and Electromagnetism, University of Seville, 41012 Seville, Spain.

D. R. Jackson is with the Department of Electrical and Computer Engineering, University of Houston, Houston, TX 77204-4793 USA.

Publisher Item Identifier S 0018-9480(01)10476-X.

More recently, a semianalytical spectral-domain technique has been introduced for calculating the current on an infinite printed-circuit transmission line, due to a practical source such as a delta-gap feed on the line [2]. This technique not only allows for the calculation of the total current on the line due to the source, but it also gives a convenient physical decomposition of the current into its constituent parts. In particular, this method shows that the total current on the line due to the source is composed of one or more *bound* modes (BMs) and a *continuous spectrum* (CS) (radiation) current. The BM current is normally the desirable current, since the BM propagates without attenuation (for a lossless structure). The CS current is a current that decays with distance from the source due to radiation loss. As discussed in [3], the CS current consists of two parts: one part is the sum of one or more physical LM currents, and the other part is the sum of one or more *residual-wave* (RW) currents. Physically, the RW currents represent that part of the CS that is not channeled into an LM. The RW currents thus correspond (loosely speaking) to the line current induced by direct radiation from the source discontinuity, as opposed to an LM current, which behaves as a quasi-guided mode.

For an open structure such as a microstrip, two types of LMs may exist: one that leaks into a surface wave and one that also leaks into space. The first type is obtained from a spectral-domain solution in which the path of integration in the transverse wavenumber plane detours around only the surface-wave pole singularities in the complex plane [1], [4]–[8]. The second type of solution comes from a path that detours around the surface-wave poles and through the branch cuts [4]–[6], [8]. Furthermore, two types of residual waves (RW) may exist. One type (referred to here as the surface-wave type) propagates from the source with the wavenumber of a surface wave and decays with distance as $1/z^{3/2}$ [3]. In addition, there is a free-space type of RW that propagates with the wavenumber of free space and decays with distance as $1/z^2$ [9].

The goal of the present work is to examine, for the first time, the nature of the current excitation from a practical source on an open microstrip line and to establish the mechanisms by which spurious transmission effects occur at high frequencies.

II. Analysis

A 1-V delta-gap source on an infinite microstrip line is shown in Fig. 1. For a narrow line, the surface current on the line is primarily in the longitudinal direction and can be written as

$$J_{sz}(x, z) = I(z)\eta(x) \tag{1}$$

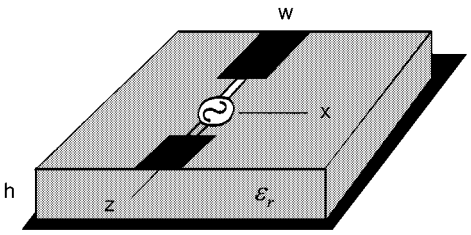

Fig. 1. Geometry of an infinite microstrip line fed by a gap source at $z = 0$.

where $I(z)$ is the current on the line and the function $\eta(x)$ describes the transverse shape of the current across the width of the line, taken as

$$\eta(x) = \frac{1}{\pi\sqrt{(w/2)^2 - x^2}} \tag{2}$$

where w is the width of the line. The line is excited by the gap source at $z = 0$. The field of the impressed gap source is taken to be

$$E_z^{\text{gap}} = \frac{1}{\Delta}, \qquad |z| < \Delta/2 \tag{3}$$

where Δ is the width of the gap source.

The electric-field integral equation (EFIE) is enforced, which states that the field due to the strip current is equal to the impressed gap field. The EFIE is enforced by applying a Galerkin method in the spectral domain, which yields a closed-form solution for the Fourier transform of the strip current. The details, which are described in [2], are omitted here. The result is

$$\tilde{I}(k_z) = \frac{2\pi\tilde{E}_z^{\text{gap}}(k_z)}{\displaystyle\int_{C_x} \tilde{G}_{zz}(k_x, k_z)\tilde{\eta}^2(k_x)\,dk_x}. \tag{4}$$

In this result, $\tilde{G}_{zz}(k_x, k_z)$ is the zz component of the spectral-domain Green's function for the field at $y = 0$ due to a source at $y = 0$. The one-dimensional (1-D) Fourier transform of the transverse shape function with respect to the x-direction, $\tilde{\eta}(k_x)$, appears in the denominator. For the shape function in (2), the transform is $J_0(k_x w/2)$, where J_0 is the zeroth-order Bessel function. The 1-D Fourier transform of the impressed gap field, with respect to the z (longitudinal) direction appears in the numerator. For the pulse-function gap field assumed here, the transform is $\text{sinc}(k_z\Delta/2)$, where $\text{sinc}(u) \equiv \sin(u)/u$.

Ideally, the width of the gap source tends to zero in order to approximate a delta-function source, in which case the Fourier transform of the gap field is unity. However, for numerical purposes, the width is taken as a finite, small number, typically 0.05 λ_0. (Allowing for a finite gap width makes the Fourier transform of the impressed gap field converge faster.) The width of the gap source has little effect on the current $I(z)$ for distances greater than several gap widths from the source.

The strip current is obtained through an inverse Fourier transform as

$$I(z) = \frac{1}{2\pi}\int_{C_z} \tilde{I}(k_z)e^{-jk_z z}\,dk_z. \tag{5}$$

The path of integration C_z in the inverse transform is along a Sommerfeld-type path in the k_z plane, as shown in Fig. 2(a). In the complex k_z plane, pole and branch-point singularities occur, and the path C_z is deformed around them. Poles in the k_z plane appears at the wavenumbers of the guided modes on the microstrip line. In fact, the denominator term in (4), when set to zero, is a transcendental equation for the wavenumber k_z of the guided-wave modes of propagation. The BM of propagation (the desired mode used for normal signal transmission) has a real wavenumber, for lossless structures. Hence, a BM pole appears on the real axis of the k_z plane at $k_z = \pm k_z^{\text{BM}}$, as shown in Fig. 2(a).

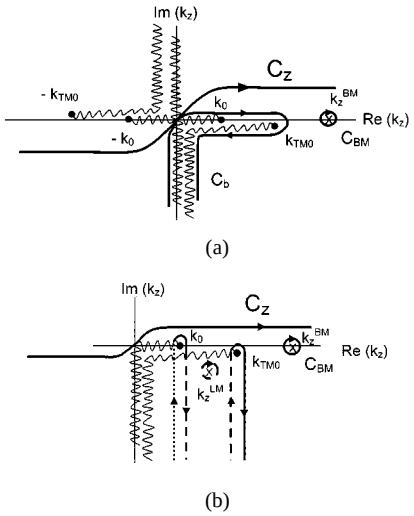

Fig. 2. (a) Complex k_z plane, showing the original path of integration C_z, an integration path C_b around the branch cuts, and a residue path C_{BM} around the BM pole. (b) Complex k_z plane, showing the path deformation to a set of vertical SDPs, a residue path around a captured LM pole k_z^{LM}, and a residue path C_{BM} around the BM pole.

The discussion of the branch points in the k_z plane is a more complicated issue, which is discussed carefully in [2] and [8]. To summarize, branch points appear in the k_z plane because the integral in the denominator of (4) is not a unique function of k_z, and this in turn is because the path of integration in the transverse wavenumber (k_x) plane is not unique. For example, there are surface-wave pole singularities (coming from the spectral-domain Green's function) in the k_x plane. The path of integration may be deformed either above or below these pole singularities [4]–[8]. This is, in fact, how the spectral-domain method allows for the solution of different types of LMs, which leak into different combinations of surface-wave modes [7]. Assuming that only the TM_0 surface-wave mode is above cutoff, a single pair of surface-wave type branch points appear on the real axis, at $k_z = \pm k_{\text{TM}_0}$, where k_{TM_0} is the wavenumber of the TM_0 surface-wave mode. These branch points are shown in Fig. 2(a). Sommerfeld (hyperbolic) branch cuts from these branch points are chosen for simplicity.

As explained in [8], a pair of branch points also appears in the k_z plane at $k_z = \pm k_0$, and these are referred to as the free-space branch points. The free-space branch points arise because of the fact that the path of integration in the k_x plane [for the denominator integral of (4)] may stay on the top sheet of the k_x plane, or it may detour through the branch cuts that appear in the k_x plane (due to the fact that the spectral-domain Green's function is for a open structure) [4]–[6], [8]. These choices of path correspond to modal solutions that either do not leak into free space, or that do, respectively. The free-space branch points on the real

axis are shown in Fig. 2(a), where once again Sommerfeld (hyperbolic) branch cuts have been chosen.

Hence, in summary, the two different types of branch points in the *longitudinal wavenumber* (k_z) plane arise from the different types of paths that are possible in the *transverse wavenumber* (k_x) plane. More details are given in [2] and [8].

The original path of integration C_z in Fig. 2(a) may be deformed into a path C_b that goes around the TM_0 and k_0 branch cuts in the lower half plane, together with a residue path C_{BM} around the BM pole on the positive real axis. The residue path around the BM pole yields a residue contribution to (5) that defines the launching amplitude A_{BM} of the BM current from the gap source. The BM current has the form

$$I_{\mathrm{BM}}(z) = A_{\mathrm{BM}} e^{-jk_z^{\mathrm{BM}}|z|}. \tag{6}$$

Hence, the BM current propagates equally in both directions away from the source, without attenuation (assuming that the wavenumber k_z^{BM} is real, for a lossless substrate).

The integration around the branch cuts, path C_b in Fig. 2(a), defines the *CS current* [10], [11], or radiation current, on the line induced by the gap source. The CS current is something that is not predicted by simple transmission-line theory (which accounts for only the BM), but is a consequence of the full-wave modeling of the complete current spectrum due to the gap source. The CS current generally increases in magnitude as the frequency increases.

It is well known that LMs may exist on printed- circuit lines such as a microstrip at high frequencies [1]. Any LMs that are excited by the gap source are automatically included as part of the CS. However, it is convenient to decompose the CS current into a form that explicitly shows the contribution from the LMs. This can be accomplished by using the path deformation shown in Fig. 2(b). The original path C_z in Fig. 2(a) has been deformed into a set of vertical paths that descend from the TM_0 and k_0 branch points on the positive real axis, as shown. These paths are referred to as steepest descent paths (SDPs), since along such vertical paths the exponential term in (5) decays as rapidly as possible, which allows for a convenient asymptotic evaluation of the integrations along these paths [3]. In deforming to the SDP paths in Fig. 2(b), the BM pole on the positive real axis is captured, as it was in Fig. 2(a). In addition, an LM pole may be captured, depending on which sheet of the k_z plane the pole is located. For example, consider an LM pole that is located on the principle sheet of the k_0 branch point, but the bottom sheet of the TM_0 branch point. Such a pole corresponds to a path of integration in the k_x plane that detours around the surface-wave poles, but does not cross the branch cuts. The corresponding LM leaks into the TM_0 surface wave of the grounded substrate, but not into space. Such a pole is captured by the SDP path deformation if it lies in the region $k_0 < \mathrm{Re}(k_z) < k_{\mathrm{TM}_0}$. That is, the pole is captured if the corresponding LM is a fast wave with respect to the TM_0 surface wave, but a slow wave with respect to free space. Such an LM is said to be a physical mode, which satisfies the path consistency condition (PCC) [7]. (In [7], the PCC was originally referred to as the "condition for leakage.") That is, the path of integration is the k_x plane used to determine the LM is physically consistent with the value of the phase constant $\beta = \mathrm{Re}(k_z)$ that results from using this path.

By means of this SDP deformation, the CS current is resolved into a sum of physical LMs (modes that satisfy the PCC, corresponding to the LM poles that are captured by the SDP path deformation) together with the currents that result from the integrations along the TM_0 and k_0 SDPs. The LM current corresponding to an LM pole that is captured has the form

$$I_{\mathrm{LM}}(z) = A_{\mathrm{LM}} e^{-jk_z^{\mathrm{LM}}|z|} \tag{7}$$

where the pole residue defines the launching amplitude A_{LM}.

The currents that arise from the integrations along the vertical SDP paths are referred to as RW currents [3]. The TM_0 and k_0 RW currents do not have a closed-form expression; these currents must be evaluated numerically by integrating along the SDP paths. However, it is possible to asymptotically evaluate these currents for large z [3]. The results show that the TM_0 RW current behaves as

$$I_{\mathrm{RW}}^{\mathrm{TM}_0}(z) \sim A_{\mathrm{RW}}^{\mathrm{TM}_0} \frac{e^{-jk_{\mathrm{TM}_0}|z|}}{(k_{\mathrm{TM}_0}|z|)^{3/2}}. \tag{8}$$

The TM_0 RW current thus propagates asymptotically with the wavenumber of the TM_0 surface-wave mode and decays with distance along the line from the source as $z^{-3/2}$. The amplitude $A_{\mathrm{RW}}^{\mathrm{TM}_0}$ can be determined from an asymptotic analysis [3], although the result is not important here (since only results for the exact RW currents, obtained by numerical integration, will be presented). For the k_0 RW current, an asymptotic analysis reveals that the behavior is [9]

$$I_{\mathrm{RW}}^{k_0}(z) \sim A_{\mathrm{RW}}^{k_0} \frac{e^{-jk_0|z|}}{(k_0|z|)^2}. \tag{9}$$

The k_0 RW current thus propagates asymptotically with the wavenumber of free space and decays along the line as z^{-2}.

Loosely speaking, the TM_0 RW current corresponds to the current on the strip that is induced by the direct radiation from the source into the TM_0 surface-wave mode, which interacts with the conducting strip. Similarly, the k_0 RW current is that current induced by direct space-wave radiation from the source.

Depending on the frequency, the substrate permittivity, and the strip width, different components of the CS current may be dominant. In some cases, a physical LM may dominate the CS current, while in other cases one or more of the RW currents may dominate. Results are presented in the next section to explore, for the first time, the nature of the current on a microstrip line excited by a gap source at high frequencies. Although the results are for a gap source only, it is expected that many of the general conclusions will remain valid for other types of sources or discontinuities on a microstrip line.

Regarding the numerical solution method, one additional point should be mentioned. The analysis described above assumed only longitudinal current on the microstrip line and further assumed that the longitudinal current is described by a single shape function or basis function in the transverse direction. This allowed for a simplified discussion of the analysis; however, in the numerical results, both longitudinal and transverse currents were actually allowed, and multiple basis functions were used for both, in the form of the Maxwellian profile function $\eta(x)$ multiplied by a corresponding Chebyshev polynomial series. This ensures accuracy, even at high frequencies. The use of multiple basis functions is also necessary to

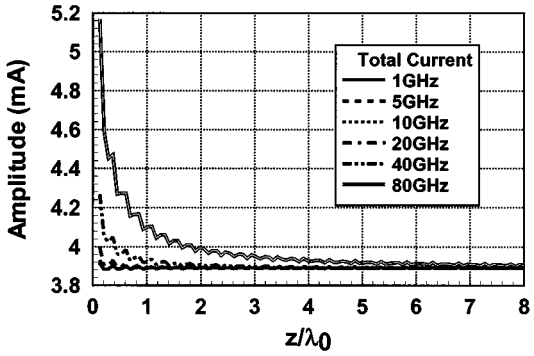

Fig. 3. Total strip current versus distance from the source, for a microstrip line with an air substrate. $w = h = 1.0$ mm. Results are shown for various frequencies.

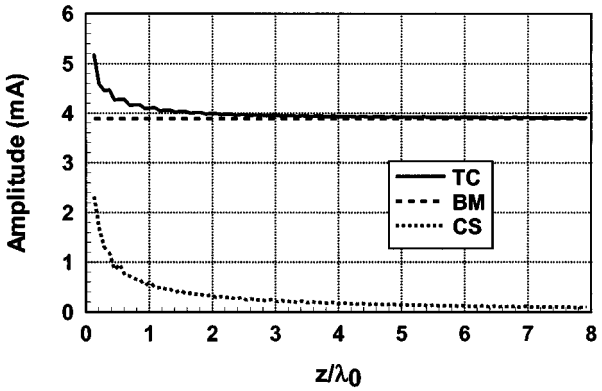

Fig. 4. Total strip current for the same microstrip line with an air substrate at 80 GHz, and the BM and CS currents that make up the total current.

properly include the effects of higher order LMs, which have a current variation across the strip that is not approximated by the quasi-TEM shape function $\eta(x)$ in (2).

III. Results

Results are presented in this section for the current $I(z)$ on a microstrip line due to the gap–source excitation, in order to study the spurious effects that may occur at high frequencies. The total strip current is resolved into the BM and CS currents to examine the source of the spurious effects. The CS current is further resolved into a physical LM current (if a physical LM exists) plus the TM_0 and k_0 RW currents to aid in the physical interpretation. In all of the cases presented, the only physical LM that is found to exist is one that leaks into the TM_0 surface-wave mode, and not into space. Such an LM is physical and hence is included in the composition of the CS current, if $k_0 < \mathrm{Re}(k_z) < k_{\mathrm{TM}_0}$. If a physical LM exists, the CS current consists of the LM current together with the TM_0 and k_0 RW currents. If no physical LM exists, the CS current is simply the sum of the two RW currents. At very high frequencies, the TE_1 surface wave may be above cutoff, and in this case a TE_1 RW current is also included in the CS current. Results are presented to show the effects of frequency, substrate permittivity, and strip width on the current, and to examine the severity of the spurious effects caused by the CS current. The decomposition of the CS current into its constituent parts is also used to investigate the nature of the CS current and to show the underlying cause of the spurious effects.

A. Air Substrate

The simplest case of a microstrip line on an air substrate ($\varepsilon_r = 1$) is considered first. The dimensions are $w = h = 1$ mm. In this case, the only mode of propagation on the microstrip line is a BM that is TEM. Since there is no substrate, there is no TM_0 surface wave, and also no TM_0 RW current. Therefore, the complete current spectrum excited by the gap source consists of a bound TEM mode (the desired mode) and a k_0 RW current. A plot of the current on the line versus normalized distance z/λ_0 from the source is shown in Fig. 3, for various frequencies ranging from low frequency to very high frequency. It is seen that, far from the source, the current plots flatten out as expected, indicating that the current is primarily that of the bound TEM mode. Near the source, the currents exhibit a very noticeable perturbing effect, due to the k_0 RW current. The effects of the k_0 RW increase with frequency, becoming quite severe at very high frequencies. One of the interesting features of the current plots is that they all exhibit a monotonic decreasing behavior with distance from the source and do not show any oscillations characteristic of the situation where two waves are interfering. This is because the bound TEM mode and the k_0 RW currents both propagate with the same wavenumber, namely that of free space. The spurious effects of the k_0 RW become severe after about 40 GHz, for which $h/\lambda_0 = 0.13$. Hence, spurious effects are avoided when using an air (or very low permittivity) substrate by keeping the substrate thickness less than about a tenth of a wavelength.

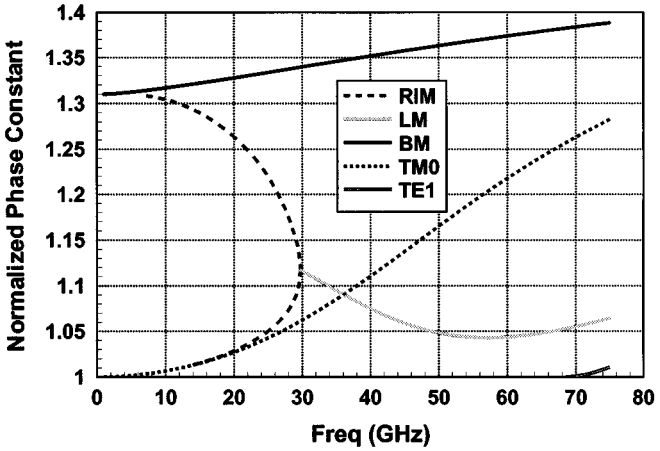

Fig. 5. Normalized phase constants (normalized by k_0) versus frequency, for a microstrip line with a moderate substrate permittivity ($\varepsilon_r = 2.2$) and a small strip width. $w = 0.333$ mm, $h = 1.0$ mm. The BM is shown along with the LM and the TM_0 and TE_1 surface-wave modes. At low frequency there is no LM, only a pair of improper real modes (RIM).

Fig. 4 shows a plot of the total strip current at 80 GHz, along with its constituent parts, the BM (TEM) current and the CS current. Although the two currents propagate with the same wavenumber, there is a constant phase difference between them, and hence the magnitude of the total current is not simply the sum of the two individual current magnitudes.

B. Moderate Permittivity Substrate

Next, results are presented for the case of a moderate permittivity substrate, $\varepsilon_r = 2.2$, for several different value of w/h, corresponding to different characteristic impedances. The substrate thickness is $h = 1.0$ mm in all cases. Fig. 5 shows the dispersion plot for a narrow line, with $w/h = 0.333$. A plot of

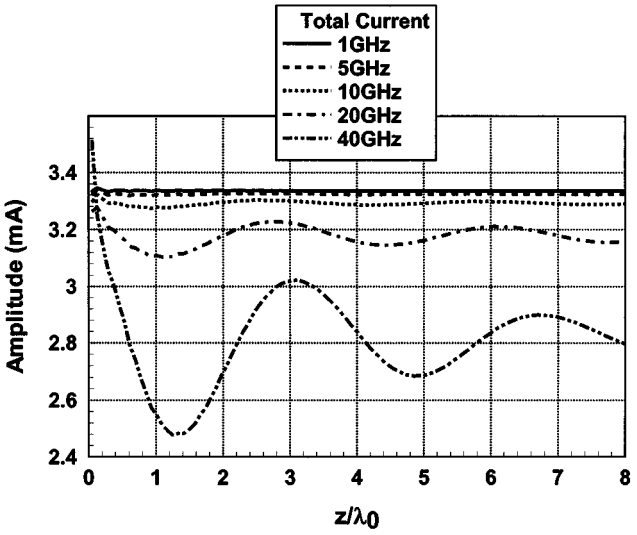

Fig. 6. Total strip current versus distance from the source, for the case of Fig. 5. Results are shown for various frequencies.

the normalized phase constant of the BM is shown, along with a plot for the LM. Also, for reference, a plot of the normalized phase constants for the TM_0 and TE_1 surface-wave modes of the grounded substrate are included. It is observed that leakage first begins at 30 GHz. Above this frequency, an LM with a complex propagation wavenumber exists on the microstrip line. The LM is an EH_0 mode, meaning that the transverse profile of the current closely resembles the quasi-TEM shape function $\eta(x)$ in (2). Below this frequency there is no LM, only a pair of improper real modes (modes that are improper, but with a real propagation wavenumber). The LM becomes physical above about 35 GHz, where it crosses the TM_0 dispersion line to become a fast wave with respect to the TM_0 surface wave.

Fig. 6 shows the total current on the strip versus normalized distance from the source, for various frequencies. As for the case of an air substrate, the general conclusion is that spurious effects increase with increasing frequency. In this case, however, the spurious effects take the form of oscillations in the total current, due to interference between the BM current and the CS current. The oscillations are due to the fact that the BM and CS currents no longer propagate down the line with the same wavenumber.

Fig. 7 shows the dispersion plots for the case of a moderate strip width, $w/h = 1.0$. Comparing with Fig. 5, it is seen that leakage begins at a lower frequency for a wider strip, although the lowering in frequency is not dramatic. Fig. 8 shows the current on the strip at various frequencies, for the case of moderate strip width. Comparing with Fig. 6, it is seen that the level of spurious oscillations is roughly the same, although the overall level of the current is higher for the wider strip case. This is because a wider strip corresponds to a smaller characteristic impedance, and hence the BM is excited with a larger amplitude in the wider strip case of Fig. 8. However, the CS is also excited with a larger amplitude, giving roughly the same level of oscillations in the total current.

Fig. 9 gives the dispersion behavior for a wide strip case, having $w/h = 3.0$. It is seen that the trend of a lower leakage frequency continues, with leakage now beginning at about 23 GHz. The current plots in Fig. 10 show a continuing increase

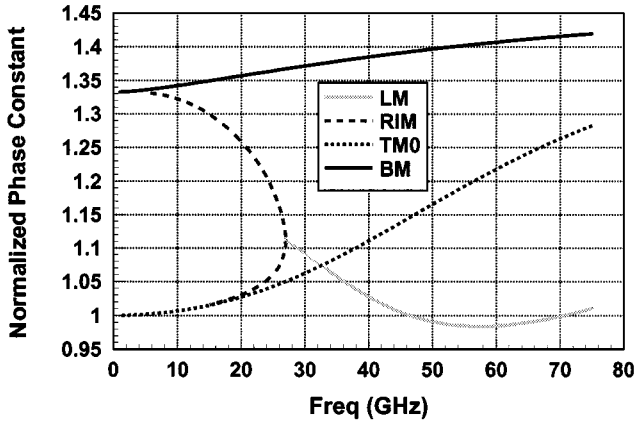

Fig. 7. Normalized phase constants (normalized by k_0) versus frequency, for a microstrip line with a moderate substrate permittivity ($\varepsilon_r = 2.2$) and a moderate strip width. $w = 1.0$ mm, $h = 1.0$ mm. The BM is shown along with the LM and the TM_0 surface-wave mode. At low frequency there is no LM, only a pair of improper real modes (RIM).

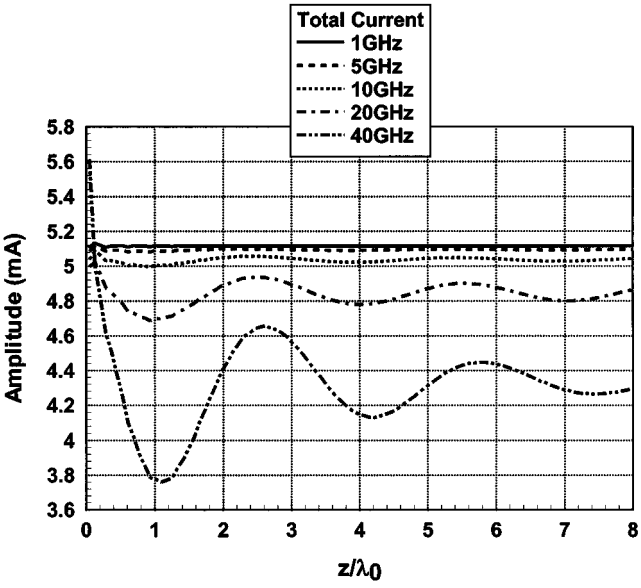

Fig. 8. Total strip current versus distance from the source, for the case of Fig. 7. Results are shown for various frequencies.

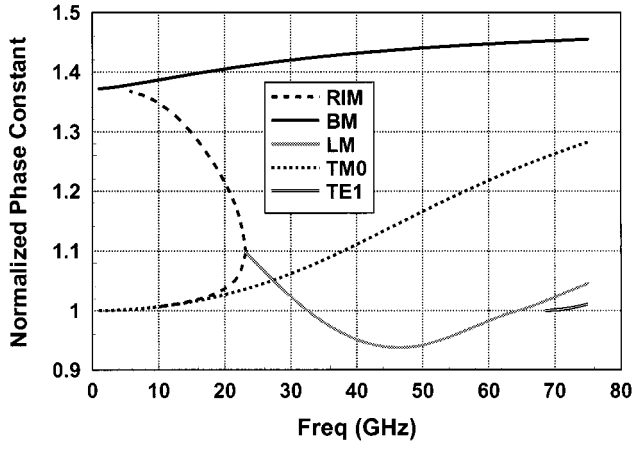

Fig. 9. Normalized phase constants (normalized by k_0) versus frequency, for a microstrip line with a moderate substrate permittivity ($\varepsilon_r = 2.2$) and a large strip width. $w = 3.0$ mm, $h = 1.0$ mm. The BM is shown along with the LM and the TM_0 and TE_1 surface-wave modes. At low frequency there is no LM, only a pair of improper real modes (RIM).

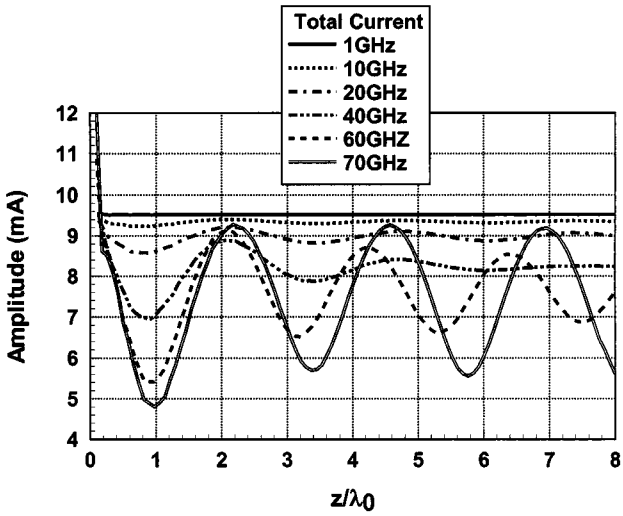

Fig. 10. Total strip current versus distance from the source, for the case of Fig. 9. Results are shown for various frequencies.

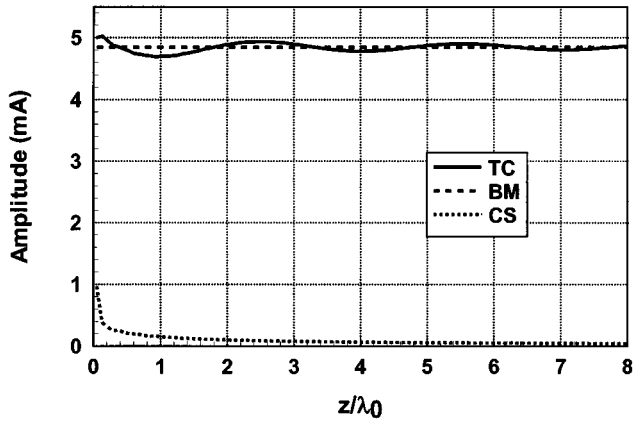

(a)

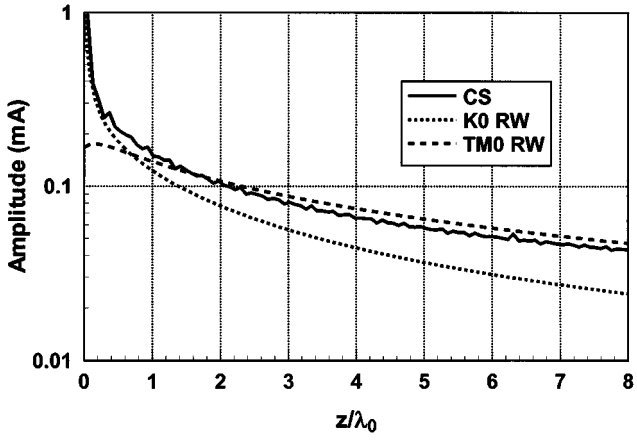

(b)

Fig. 11. Strip currents for the case of a moderate substrate permittivity ($\varepsilon_r = 2.2$) and moderate strip width ($w = h = 1.0$ mm) at 20 GHz. (a) Total current and its constituent parts, the BM and CS currents. (b) CS current and its constituent parts, the TM_0 RW and k_0 RW currents.

in the overall current level, with a spurious oscillation level that is similar to the other strip width cases.

In Fig. 11, the current is investigated in more detail for the moderate strip width case ($w/h = 1$), at a frequency of 20 GHz. Fig. 11(a) shows the total current and its constituent parts, the BM and CS currents. Fig. 11(b) shows the CS current resolved into its constituent parts, the k_0 RW current and the TM_0 RW current. There is no physical LM at this frequency (see Fig. 7) so the CS current is simply the sum of the two RW currents. The TM_0 RW current is the stronger of the two RWs, although the amplitudes of both waves are somewhat comparable.

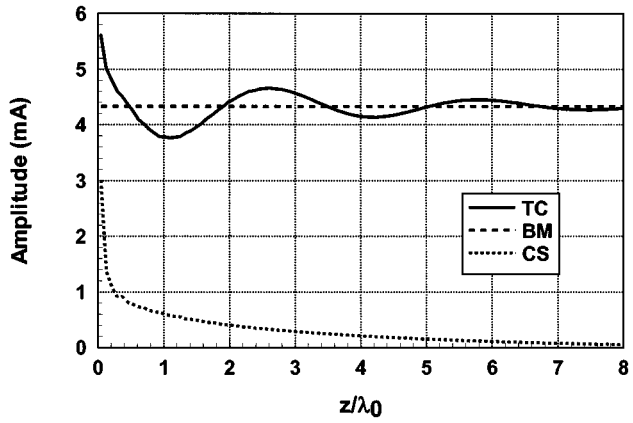

(a)

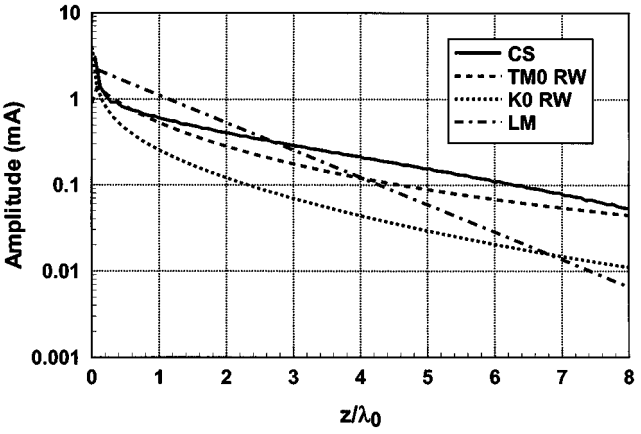

(b)

Fig. 12. Strip currents for the case of a moderate substrate permittivity ($\varepsilon_r = 2.2$) and moderate strip width ($w = h = 1.0$ mm) at 40 GHz. (a) Total current and its constituent parts, the BM and CS currents. (b) CS current and its constituent parts, an LM current together with TM_0 RW and k_0 RW currents.

At 40 GHz, the situation changes in that a physical LM now exists (see Fig. 7). At this higher frequency, the oscillations in the total strip current are larger, as seen in Fig. 12(a). This is because the magnitude of the CS current has increased with frequency. In Fig. 12(b), the CS current is shown with its three components, the LM current, the k_0 RW current, and the TM_0 RW current. Close to the source, the LM current is the strongest. However, because the LM current decays exponentially with distance, the two RW currents become dominant for larger distances. The TM_0 RW current is the more dominant of the two, as for the 20-GHz case. The presence of the physical LM causes the level of spurious oscillation to be quite significant close to the source in the 40-GHz case, much larger than in the 20-GHz case. Further away from the source the level of spurious oscillation is still slightly larger in the 40-GHz case, but the increase is not as dramatic.

In the previous cases, the TM_0 RW current was dominant over the k_0 RW current. This appears to be the usual situation,

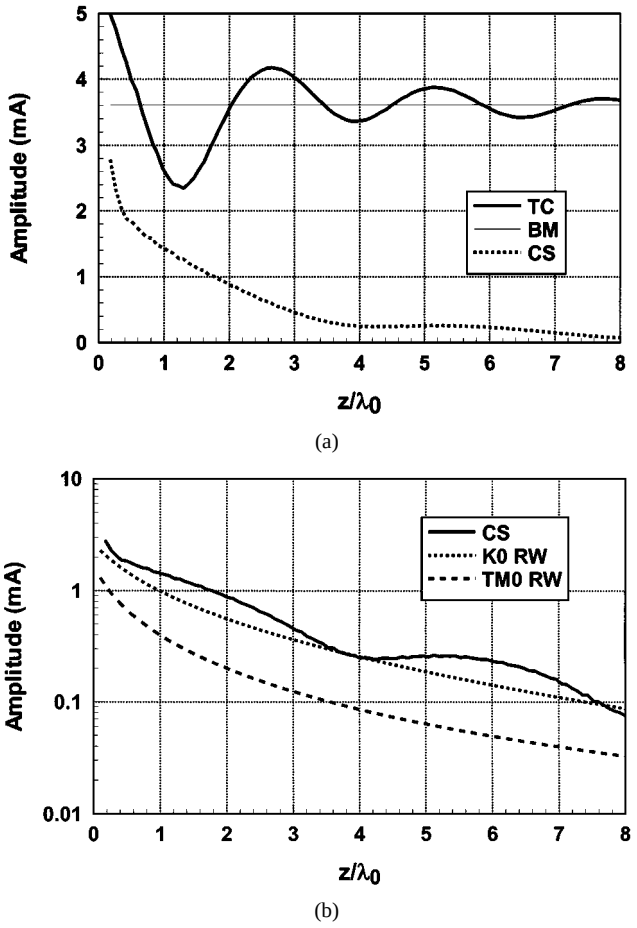

Fig. 13. Strip currents for the case of a moderate substrate permittivity ($\varepsilon_r = 2.2$) and moderate strip width ($w = h = 1.0$ mm) at 68.418 GHz. (a) Total current and its constituent parts, the BM and CS currents. (b) CS current and its constituent parts, the TM_0 RW and k_0 RW currents.

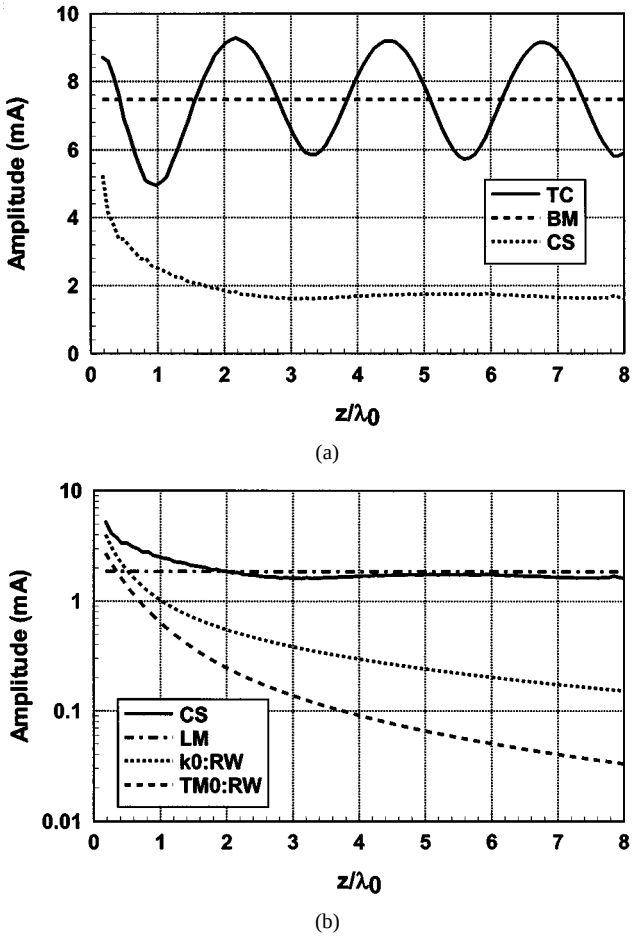

Fig. 14. Strip currents for the case of a moderate substrate permittivity ($\varepsilon_r = 2.2$) and wide strip width ($w = 3.0$ mm, $h = 1.0$ mm) at 67.37 GHz. (a) Total current and its constituent parts, the BM and CS currents. (b) CS current and its constituent parts: an LM current together with TM_0 RW and k_0 RW currents.

at least for a moderate permittivity substrate. However, it is possible to find exceptions. In Fig. 13, a frequency of 68.418 GHz was chosen. At this particular frequency, the TE_1 surface-wave mode of the substrate is at cutoff. Fig. 13(a) shows the expected trend of increased oscillations due to a stronger CS current at this higher frequency. Even more interesting, however, is the fact that, at this particular frequency, the k_0 RW current now dominates the TM_0 RW current. This is because the TE_1 surface-wave mode of the substrate is at cutoff, and therefore the wavenumber of the TE_1 surface wave is k_0. In the k_z plane of Fig. 2, this has the effect of creating a TE_1 branch point on the real axis at k_0, so that the TE_1 branch point coincides with the k_0 branch point. The result is a strong k_0 RW current, as seen in Fig. 13(b).

Another interesting situation occurs in Fig. 14, where a wide strip ($w/h = 3.0$) is used at a high frequency of 67.37 GHz. This frequency is chosen from the formula

$$k_0\sqrt{\varepsilon_r}w = 2\pi \tag{10}$$

which is an approximate equation that predicts the cutoff frequency of the EH_2 mode, assuming perfect magnetic walls on the sides. (This mode has a current profile that is an even function about the center of the strip, with approximately one cycle of variation across the strip width.) Equation (10) accurately predicts the EH_2 mode cutoff frequency only when the strip width is very wide (e.g., $w/h > 10$). Nevertheless, at the frequency predicted by this equation (67.37 GHz), a leaky EH_2 mode with a very small attenuation constant exists. Hence, at

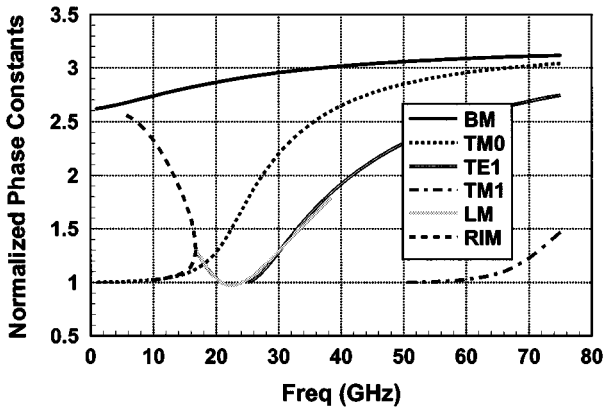

Fig. 15. Normalized phase constants (normalized by k_0) versus frequency, for a microstrip line with a high substrate permittivity ($\varepsilon_r = 10.2$) and a moderate strip width ($w = h = 1.0$ mm). The BM is shown along with an LM and the TM_0, TE_1, and TM_1 surface-wave modes. At low frequency there is no LM, only a pair of improper real modes (RIM).

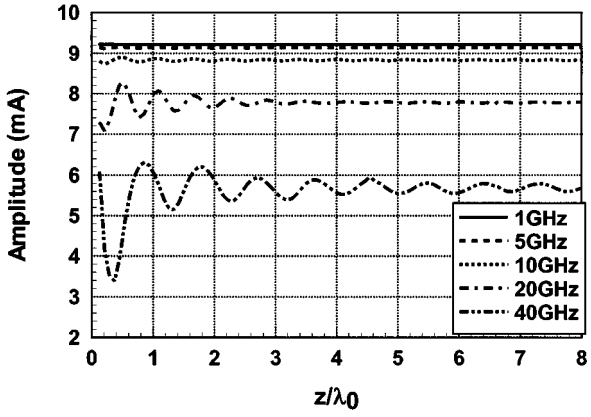

Fig. 16. Total strip current versus distance from the source, for the microstrip line of Fig. 15 at various frequencies.

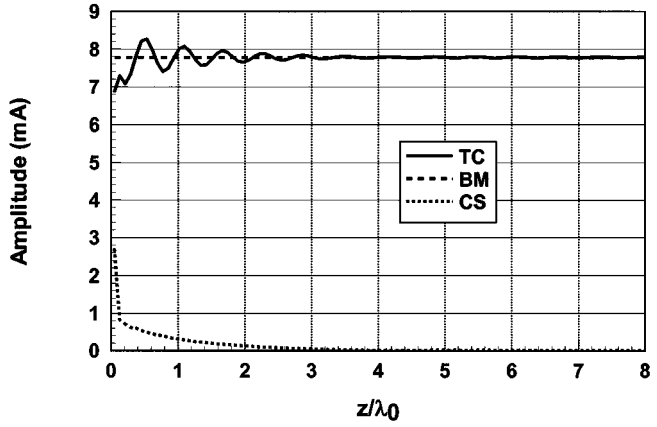

(a)

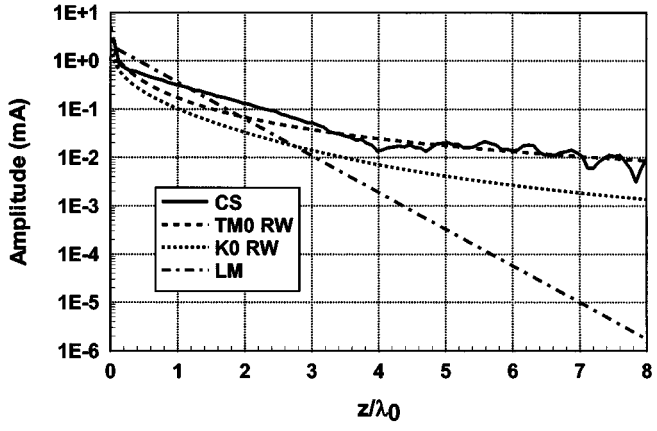

(b)

Fig. 17. Strip currents for the high-permittivity case of Fig. 16 at 20 GHz. (a) Total current and its constituent parts, the BM and CS currents. (b) CS current and its constituent parts: an LM current together with TM_0 RW and k_0 RW currents.

this frequency, the source excites a very weakly attenuated EH_2 LM on the microstrip. This causes the CS current to remain almost flat with distance as the distance from the source increases, as seen in Fig. 14(a). This in turn causes the oscillation in the total strip current to persist almost without decay out to very large distances. In Fig. 14(b), the resolution of the CS current into its parts clearly shows the dominance of the EH_2 LM.

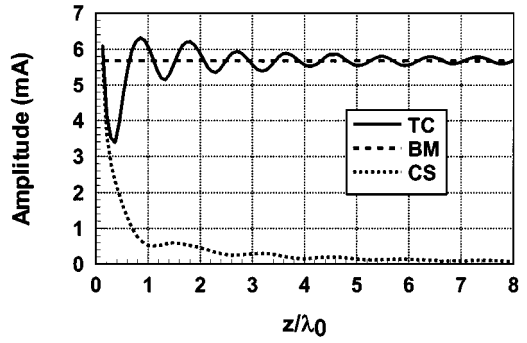

(a)

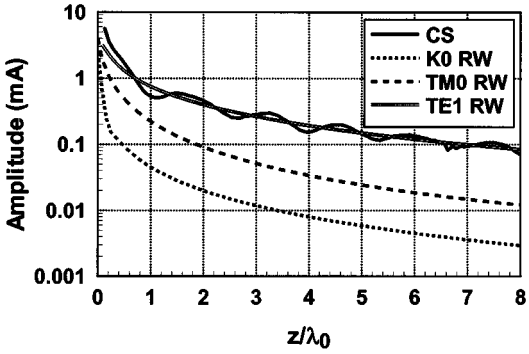

(b)

Fig. 18. Strip currents for the high-permittivity case of Fig. 16 at 40 GHz. (a) Total current and its constituent parts, the BM and CS currents. (b) CS current and its constituent parts: TM_0 RW TE_1 RW, and k_0 RW currents.

Although the EH_1 mode (the first higher order mode on the microstrip) has a lower cutoff frequency than the EH_2 mode, the EH_1 mode is an odd mode and is not excited by the gap source (which is an even function about the center of the strip).

C. High Permittivity Substrate

Fig. 15 shows the dispersion behavior for a microstrip with a high permittivity substrate ($\varepsilon_r = 10.2$) and a moderate strip width ($w/h = 1.0$). Comparing with Fig. 7, it is seen that the higher permittivity has lowered the frequency at which leakage begins. Fig. 16 shows the current versus distance from the source for this high-permittivity case. The level of spurious oscillations in the strip current increases with frequency, as for the moderate-permittivity case of Fig. 8.

Fig. 17(a) shows the total strip current at 20 GHz for the case of Fig. 16 along with its components, the BM and CS currents. In Fig. 17(b) it is seen that a physical EH_0 LM dominants the CS current near the source (although the k_0 RW and TM_0 RW currents are not negligible). Due to the exponential decay of this LM, the oscillations in the total strip current die out fairly quickly with distance, leaving only a very small amount of oscillations due to the relatively weak RW currents.

At 40 GHz, the oscillations become stronger, as seen in Fig. 18. Interestingly, this is not due to the excitation of an LM, as was the case for the moderate permittivity substrate at 40 GHz. At 40 GHz, there is no physical LM in the high permittivity case, but there are three RW currents: the k_0 RW current, the TM_0 RW current, and the TE_1 RW current (since the TE_1 surface wave is above cutoff). (The LM shown in

Fig. 15 leaks only in the TM_0 surface wave; this mode is not physical at 40 GHz since the phase constant is less than that of the TE_1 surface wave.) The CS current is quite large due to the strong excitation of the TE_1 RW current, which is the dominant contributor to the CS current. Since the spurious oscillations are mainly due to a RW, the oscillations die out fairly slowly with distance.

IV. Conclusion

High-frequency spurious effects in the current excited by a gap source on a microstrip line have been investigated. The gap source serves as a canonical model for feeds or other discontinuities on the line. At high frequencies, the total current on the line varies significantly with distance z from the source, departing markedly from an ideal flat response, as predicted from simple transmission line theory. This deviation is due to interference between the BM of propagation (the desired mode) and a *CS* current. The CS current (also loosely called a radiation current) increases in magnitude with frequency, and hence the level of the spurious effects increases with frequency. The CS current is the sum of any physical LM currents (if any exist) plus "*RW*" currents. There are two types of RW currents for an open structure such as microstrip: a surface-wave RW current and a k_0 (free-space) RW current. At moderate frequencies the only surface-wave RW current is the TM_0 one, but at very high frequencies a TE_1 RW current will also exist (whenever the TE_1 surface-wave on the grounded substrate is above cutoff).

When the substrate is air, the BM of propagation is a TEM mode, and there is no LM. There is also no TM_0 RW current. Therefore, the CS consists entirely of the k_0 RW current, which propagates with the wavenumber of free space, the same as for the bound TEM mode. The total strip current therefore shows a monotonic behavior, decreasing with distance from the source.

When the substrate has a moderate permittivity (a relative permittivity of 2.2 was used in the results) and a moderate strip width, the total current on the strip exhibits spurious oscillations, due to interference between the BM current and the CS current. Results show that spurious effects increase with frequency and become very severe when the substrate thickness is about a tenth of a wavelength. At moderately high frequencies, the spurious effects for a moderate permittivity substrate are due mainly to the TM_0 RW and, to a lesser extent, the k_0 RW. At higher frequencies, the spurious effects are due partly to a physical EH_0 (quasi-TEM) LM in a region close to the source, but further away from the source they are mainly due once again to the TM_0 RW. At extremely high frequencies, where the TE_1 surface wave approaches cutoff, the spurious effects are mainly due to the k_0 RW.

For high-permittivity substrates (a relative permittivity of 10.2 was in the results) and moderate strip widths, the spurious effects observed at moderately high frequencies are due to an EH_0 LM near the source, and due to the TM_0 RW further away. At very high frequencies, the spurious effects are mainly due to a TE_1 RW current.

For wide strips, the results show that there is an interesting effect that may cause the spurious oscillations in the strip current to extend to very large distances from the source at high frequencies (the frequency at which this effect occurs depends on the strip width). This effect is due to the excitation of a higher-order EH_2 LM that has a small attenuation constant. Due to the small attenuation constant, the LM can propagate to very large distances before decaying significantly. Clearly, the width of the microstrip line should be chosen to avoid this effect.

References

[1] D. Nghiem, J. T. Williams, D. R. Jackson, and A. A. Oliner, "Leakage of the dominant mode on microstrip with an isotropic substrate: Theory and measurements," *IEEE Trans. Microwave Theory Tech.*, vol. 44, pp. 1710–1715, Oct. 1996.

[2] C. Di Nallo, F. Mesa, and D. R. Jackson, "Excitation of leaky modes on multilayer stripline structures," *IEEE Trans. Microwave Theory Tech.*, vol. 46, pp. 1062–1071, Aug. 1998.

[3] D. R. Jackson, F. Mesa, M. Freire, D. P. Nyquist, and C. Di Nallo, "An excitation theory for bound modes, leaky modes, and residual-wave currents on stripline structures," *Radio Sci.*, vol. 35, no. 2, pp. 495–510, Mar.–Apr. 2000.

[4] J. Boukamp and R. H. Jansen, "Spectral domain investigation of surface-wave excitation and radiation by microstrip lines and microstrip disk resonators," in *Proc. Eur. Microwave Conf.*, vol. 13, 1983, pp. 721–726.

[5] K. A. Michalski and D. Zheng, "Rigorous analysis of open microstrip lines of arbitrary cross section in bound and leaky regimes," *IEEE Trans. Microwave Theory Tech.*, vol. 37, pp. 2005–2010, Dec. 1989.

[6] N. K. Das and D. M. Pozar, "Full-wave spectral-domain computation of material, radiation, and guided wave losses in infinite multilayered printed transmission lines," *IEEE Trans. Microwave Theory Tech.*, vol. 39, pp. 54–63, Jan. 1991.

[7] D. Nghiem, J. T. Williams, D. R. Jackson, and A. A. Oliner, "Proper and improper dominant mode solutions for stripline with an air gap," *Radio Sci.*, vol. 28, no. 6, pp. 1163–1180, Nov.–Dec. 1993.

[8] F. Mesa, C. Di Nallo, and D. R. Jackson, "The theory of surface-wave and space-wave leaky mode excitation on microstrip lines," *IEEE Trans. Microwave Theory Tech.*, vol. 47, pp. 207–215, Feb. 1999.

[9] D. R. Jackson, F. Mesa, M. J. Freire, and D. P. Nyquist, "The current on a microstrip line excited from a discontinuity," in *PIERS Symp.*, Cambridge, MA, July 5–14, 2000, p. (Proc., p. 237).

[10] J. M. Grimm and P. P. Nyquist, "Spectral analysis considerations relevant to radiation and leaky modes of open-boundary microstrip transmission line," *IEEE Trans. Microwave Theory Tech.*, vol. 41, pp. 150–153, Jan. 1993.

[11] D. P. Nyquist and D. J. Infante, "Discrete higher-order leaky-wave modes and the continuous spectrum of stripline," *IEICE Trans.*, vol. E78-C, pp. 1331–1338, Oct. 1995.

[12] H. Shigesawa, M. Tsuji, and A. A. Oliner, "Conductor-backed slot line and coplanar waveguide: Dangers and full-wave analysis," in *Proc. IEEE MTT-S Int. Microwave Symp. Dig.*, 1988, pp. 199–202.

[13] M. Tsuji, H. Shigesawa, and A. A. Oliner, "Printed-circuit waveguide with anisotropic substrates: A new leakage effect," in *Proc. IEEE MTT-S Int. Microwave Symp. Dig.*, 1989, pp. 783–786.

[14] ——, "Simultaneous propagation of both bound and leaky modes on conductor-backed coplanar strips," in *Proc. IEEE MTT-S Int. Microwave Symp. Dig.*, Atlanta, GA, 1993, pp. 1295–1298.

[15] H. Shigesawa, M. Tsuji, and A. A. Oliner, "The nature of the spectral-gap between bound and leaky solution when dielectric loss is present in printed-circuit lines," *Radio Sci.*, vol. 28, no. 6, pp. 1235–1243, Nov.–Dec. 1993.

[16] J. L. Cina and L. Carin, "Mode conversion and leaky-wave excitation at open-end coupled-microstrip discontinuities," *IEEE Trans. Microwave Theory Tech.*, vol. 43, pp. 2066–2071, Sept. 1995.

[17] N. K. Das, "Power leakage, characteristic impedance and leakage-transition behavior of finite-length stub section of leaky printed transmission lines," *IEEE Trans. Microwave Theory Tech.*, vol. 44, pp. 526–536, Apr. 1996.

[18] J. Zehentner and J. Machac, "Properties of CPW in the sub-MM wave range and its potential to radiate," in *Proc. IEEE MTT-S Int. Microwave Symp. Dig.*, 2000, pp. 1061–1064.

[19] F. Mesa, A. A. Oliner, D. R. Jackson, and M. J. Freire, "The influence of a top cover on the leakage form microstrip line," *IEEE Trans. Microwave Theory Tech.*, vol. 48, no. 12, pp. 2240–2248, Dec. 2000.

Francisco Mesa (M'94) was born in Cadiz, Spain, in April 1965. He received the Licenciado and Ph.D. degrees in physics from the University of Seville, Seville, Spain, in 1989 and 1991, respectively.

He is currently an Associate Professor in the Department of Applied Physics, University of Seville. His research interests focus on electromagnetic propagation/radiation in planar lines with general anisotropic materials.

David R. Jackson (S'83–M'84–SM'95–F'99) was born in St. Louis, MO, on March 28, 1957. He received the B.S.E.E. and M.S.E.E. degrees from the University of Missouri, Columbia, in 1979 and 1981, respectively, and the Ph.D. degree in electrical engineering from the University of California at Los Angeles, in 1985.

From 1985 to 1991, he was an Assistant Professor in the Department of Electrical and Computer Engineering, University of Houston, Houston, TX. From 1991 to 1998, he was an Associate Professor in the same department, and since 1998, he has been a Professor in the same department. His current research interests include microstrip antennas and circuits, leaky-wave antennas, leakage and radiation effects in microwave integrated circuits, periodic structures, and bioelectromagnetics. He is an Associate Editor for the *International Journal of RF and Microwave Computer-Aided Engineering* and is a past Associate Editor for *Radio Science*.

Dr. Jackson is the chapter activities coordinator for the IEEE Antennas and Propagation Society (IEEE AP-S) and is the chair of the Technical Activities Committee for URSI, U.S. Commission B. He is a distinguished lecturer for the IEEE AP-S. He is a past associate editor for the IEEE TRANSACTIONS ON ANTENNAS AND PROPAGATION. He was a member of the IEEE AP-S AdCom.

Manuel J. Freire was born in Cádiz, Spain, in 1972. He received the Licenciado and Ph.D. degrees in physics from the University of Seville, Seville, Spain, in 1995 and 2000, respectively.

From 1995 to 1996, he was with the Royal Naval Observatory of the Spanish Navy, San Fernando, Cádiz, Spain. In 1996, he was with the Microwave Group, University of Seville. In 1988, he was a Visiting Researcher in the Department of Electrical and Computer Engineering, University of Houston, Houston, TX. He is currently an Assistant Professor in the Department of Electronics and Electromagnetics, University of Seville. His research interests focus on leaky-wave propagation in microstrip structures and electromagnetic propagation in planar structures with anisotropic media.